Theor Appl Climatol (2011) 103:229–237
DOI 10.1007/s00704-010-0295-6

ORIGINAL PAPER

Climate-driven chlorophyll-*a* concentration interannual variability in the South China Sea

Shilin Tang · Qing Dong · Fenfen Liu

Received: 30 September 2009 / Accepted: 10 May 2010 / Published online: 25 May 2010

Abstract Physical forcing and biological response are highly variable over a wide range of scales in the South China Sea. The present paper analyzed interannual variability of the surface chlorophyll-*a* concentration of the South China Sea using NASA standard SeaWiFS monthly products from 1997 to 2007. Time series of monthly data were first smoothed using a 12-month running mean filter. An empirical orthogonal function (EOF) analysis was performed to evaluate the interannual variability. The first EOF mode is characterized by a higher surface chlorophyll-*a* concentration in the deep basin of the South China Sea with a maximum value southwest of Luzon Strait. The corresponding time coefficient function is highly correlated with the multivariate ENSO index (MEI). The correlation coefficient is −0.61 when the time coefficient function lags the MEI by 9 months. The second EOF mode is characterized by a northwest lower chlorophyll-*a* concentration. The corresponding time coefficient function correlates with the MEI at a correlation coefficient equal to 0.88, with a lag of 1 month. The third EOF mode shows the interannual variability of the chlorophyll-*a* concentration has some relationship with Indian Ocean dipole mode as well. The link between the climate and ocean biological states in the South China Sea is due to changes in upper-ocean temperature and wind field, which influence the availability of nutrients for phytoplankton growth.

S. Tang · Q. Dong
Key Laboratory of Digital Earth,
Center for Earth Observation and Digital Earth,
Chinese Academy of Sciences,
Beijing 100101, China

S. Tang (✉)
Freshwater Institute, Fisheries and Oceans Canada,
Winnipeg, MB R3T 2N6, Canada
e-mail: Shilin.Tang@dfo-mpo.gc.ca
e-mail: sltang@ceode.ac.cn

F. Liu
LED, South China Sea Institute of Oceanology,
Chinese Academy of Sciences,
Guangzhou 510301, China

1 Introduction

Phytoplankton biomass is highly variable in space and time. The seasonal to interannual changes in phytoplankton biomass are very important components of the total variability associated with ocean biological and biogeochemical processes. The Sea Viewing Wide Field of View Sensor (SeaWiFS), launched in the fall of 1997, provides a high-quality data set of sea surface phytoplankton chlorophyll-*a* concentration of the global ocean with an unprecedented spatial coverage. SeaWiFS data have been collected for more than 10 years. The length of the SeaWiFS time series allows study of the interannual variability. These SeaWiFS data have been used in the past to evaluate various conceptual modes linking the physical and biological properties on a global scale (Legaard and Thomas 2007). A 4-year variability of the global chlorophyll-*a* concentration was used to qualify the major seasonal signals in phytoplankton biomass between 50°S and 50°N (Yoder and Kennelly 2003). Climate effects on ocean biology are reported from 1997 to 2006 of the global ocean, and a significant correspondence between the global ocean primary productivity changes and the multivariate ENSO index (MEI) was found (Behrenfeld et al. 2006).

The South China Sea is a typical marginal sea south of China, which spans 0–23°N and 100–121°E (Fig. 1). As the largest and deepest marginal sea in the tropical Pacific, it links the Indian Ocean and the Pacific Ocean, encompassing

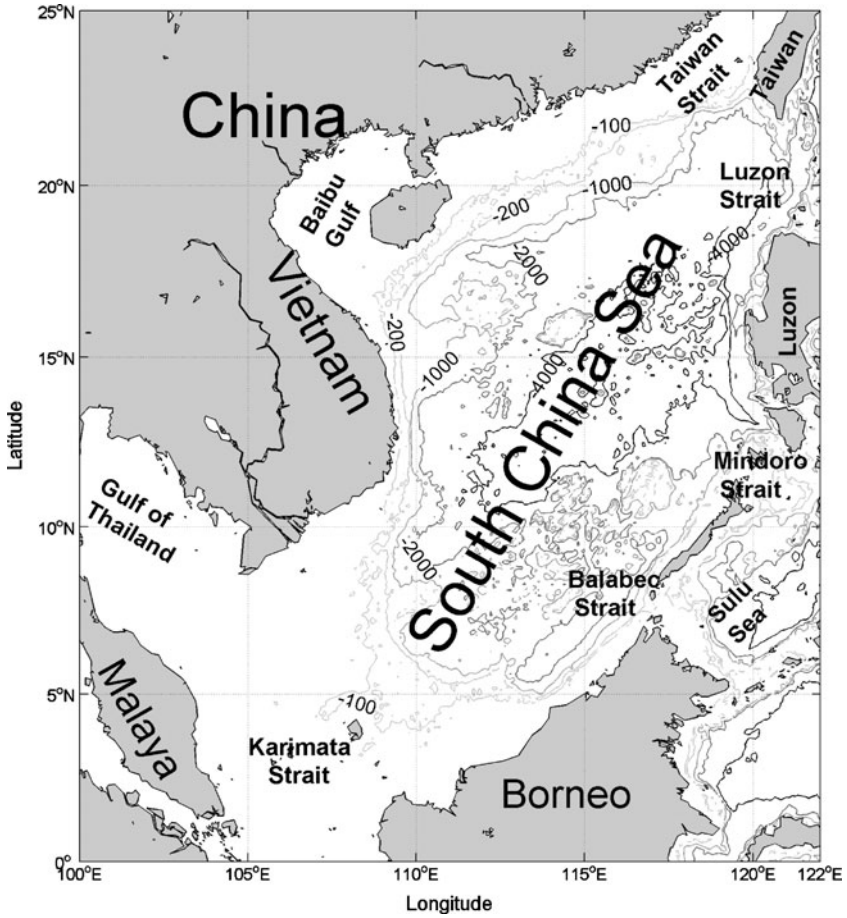

Fig. 1 Bathymetric and geographic map of the study area of this work

a portion of the Pacific Ocean stretching roughly from Singapore and the Strait of Malacca in the northwest to the Strait of Taiwan in the northeast with an area of around 3,500,000 km^2, in which about 30% of the South China Sea is deep-sea area with an average depth of 1,400 m. There are longshore currents and warm currents driven by the Kuroshio in its north, and the South China Sea plays an important role in the East Asian monsoon due to its high water temperature and large heat content in the upper ocean.

The South China Sea undergoes a pronounced seasonal variability under the influence of the East Asian summer monsoon (Wang et al. 2001; Li et al. 2009). Meanwhile, as a tropical Pacific marginal sea, the South China Sea exhibits a remarkable interannual variability. The seasonal and interannual variability of the physical environmental parameters, including sea surface temperature (SST), sea surface height, and sea surface heat flux in the South China Sea, have been widely discussed (Ho et al. 2000; Qu 2001; Li et al. 2004; Fang et al. 2006b; Han and Huang 2009; Zeng and Wang 2009). The sea surface winds, surface height, and surface temperature in the South China Sea are analyzed based on the empirical orthogonal function (EOF), and the ENSO-associated correlation patterns of them were found (Fang et al. 2006a). A double-peak evolution of the SST anomaly was found following an El Niño event (Wang et al. 2006). The variability of SST of the Vietnam coastal upwelling during the 1997–1998 ENSO event was observed by multisensor data (Kuo et al. 2004). The annual, interannual, and longer-term sea-level variations in the South China Sea are revealed, and the mechanism is discussed (Han and Huang 2009). However, the South China Sea is poorly understood in terms of its biological characteristics, despite of the work by a few investigators (Tan et al. 2006; Liu et al. 2007; Penaflor et al. 2007), which are almost concentrated on the seasonal phytoplankton variability. The seasonal variation of chlorophyll-*a* concentration in the Northern South China Sea were analyzed by Giovanni from September 1997 to August 2006, and a higher chlorophyll-*a* concentration and cooler SST in the winter bloom were indicated to link with the South China Sea winter monsoon (Shen et al. 2008). Monsoonal phytoplankton bloom in the Luzon Strait was detected with MODIS data (Penaflor et al. 2007). The chlorophyll-*a* concentration during 1998 summer in the South China Sea was the lowest among 1998 to 2005, and the jet-shape chlorophyll-*a* region offshore of the southeast Vietnam almost disappeared in that season (Zhao and Tang 2007). However, these works focused on the

seasonal phytoplankton variability or special phenomena in a small region or a short period anomaly. Up to now, the report on the understanding of interannual changes in phytoplankton abundance variability in the South China Sea has not been seen, and the mechanisms that are responsible for the South China Sea interannual phytoplankton abundance variability are not very clear.

With the availability of more than 10 years of SeaWiFS chlorophyll-*a* concentration data, this paper undertakes a worthwhile integrated analysis of the sea surface chlorophyll-*a* concentration field to provide more systematic views for the trends and interannual variability in the South China Sea. More importantly, the variability of the biomass with the El Niño/Southern Oscillation or the Indian Ocean dipole (IOD) mode has been analyzed in detail.

2 Data and methods

The data used in the present study contain the chlorophyll-*a* concentration, SST, sea wind stress curl, MEI, and IOD index.

Surface chlorophyll-*a* concentrations were obtained from the Ocean Biology Processing Group (OBPG) of the Goddard Space Flight Center (GSFC), NASA (http://oceancolor.gsfc.nasa.gov/ftp.html). It is the monthly SeaWiFS level 3 mapped products (version 5.2; Hooker and McClain 2000). The ocean color algorithm in this area is controversial. Some people regarded that the chlorophyll-*a* product is satisfiable (Zhao et al. 2005). Although a report showed the chlorophyll-*a* concentration from the SeaWiFS standard algorithm had a large discrepancy from the in situ chlorophyll-*a* concentration, the standard algorithm was regarded to overestimate the chlorophyll-*a* concentration about 1.66 times in the whole range (Tang et al. 2008). For the analysis of this work, the direct proportion relationship will not influence the result in this work. SeaWiFS products in the OBPG have been available since September 1997, but we chose the data during the period from October 1997 to December 2007, and the data of September 1997 was abandoned because the data of this month in the South China Sea are less than one third coverage. To reduce the size of the data set used in the subsequent calculation, the original data were re-binned to a $1/3 \times 1/3°$ grid using the geometric mean. The missing data in these re-binned data were then estimated using the kriging interpolation with a Gaussian semivariogram model and a fixed search radius of 3 points (Stein 1999).

The SST data used in this paper are the South China Sea subset of the AVHRR Pathfinder product version 5.0. Pathfinder is a joint NASA/NOAA project devoted to the production of global SST maps from 1985 to the present. The Pathfinder data are available at a daily/4 km time/space resolution. Here, we choose the nighttime descending monthly products. We reduce the size of the data set using the methods outlined above for the chlorophyll-*a* concentration.

The sea wind (SW) data used in this work are the Quikscat Scatterometer monthly mean field products produced by the Center for Satellite Exploitation and Research (CERSAT) at the French Institute of Research for the Exploitation of the Sea (Ifremer) (http://cersat.ifremer.fr/data/discovery/by_parameter/ocean_wind/mwf_quikscat). The data contain wind stress curl, which was derived from the wind stress using finite difference schemes. The data have a resolution of $0.5 \times 0.5°$. The data cover the period from August 1999 to October 2009.

ENSO is the largest source of the Earth's climate variability in the instrumental record. ENSO-related SST anomalies are found over many places, including the South China Sea. The strength of the ENSO is scaled using the MEI, which combines six important variables, including sea-level pressure, zonal and meridional velocity of the surface wind, SST, surface air temperature, and total cloudiness fraction of the sky. Negative values of the MEI represent the cold ENSO phase (La Niña), while positive MEI values represent the warm ENSO phase (El Niño; Wolter and Timlin 1993, 1998). The MEI data are obtained from the Climate Diagnostics Center, NOAA (http://www.cdc.noaa.gov/Correlation/mei.data).

The IOD is a coupled ocean–atmosphere phenomenon in the Indian Ocean. It is normally characterized by an anomalous cooling of SST in the southeastern equatorial Indian Ocean and an anomalous warming of SST in the western equatorial Indian Ocean. The intensity of the IOD is defined by Saji as the SST difference between the tropical western Indian Ocean (50°E–70°E, 10°S–10°N) and the tropical southeastern Indian Ocean southwest of Sumatra (90°E–110°E, 10°S–Equator; Saji et al. 1999).

For interannual variability analysis, we first filtered out the seasonal variability using a 12-month running mean at each grid point. The 12-month running mean is one of the shortest filters to remove frequencies higher than 12 months in terms of the Fourier spectrum. Thus, the amplitude modulation of the annual variation or the seasonality variability is also filtered out (Emery and Thomson 2001; Fang et al. 2006a). For avoiding the unknown errors in the EOF analysis, the first and the last 6 months of the data were discarded although they contain the strong El Niño 1997–1998 period. In addition, the MEI and the IOD index were processed using the same method to get the interannual value.

The EOF analysis is an efficient method of extracting the dominant temporal and spatial components of variability into a series of orthogonal functions or statistical modes and is used routinely in physical oceanography, atmospheric studies (Nagar and Singh 1991), and frequently in

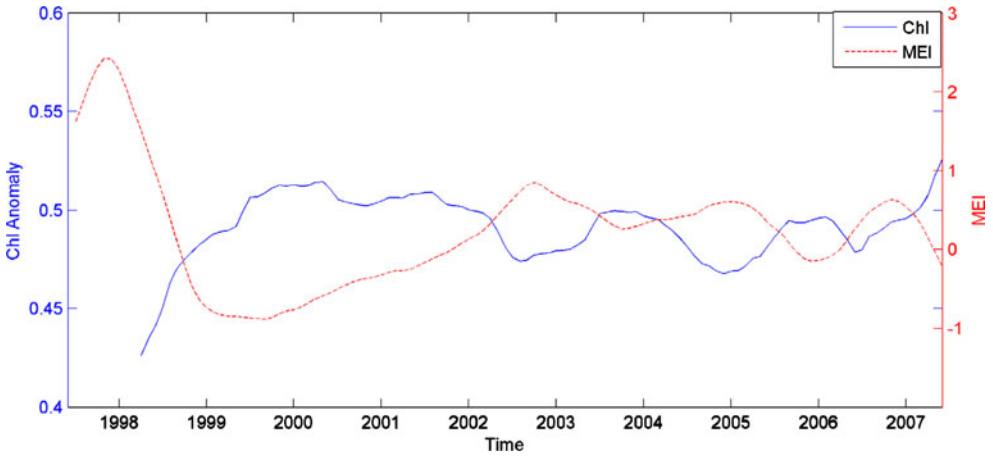

Fig. 2 The average interannual variability of the chlorophyll-*a* concentration in the South China Sea (*blue solid line*) and the multivariate ENSO index (*red dotted line*)

biological oceanography recently (Wilson and Adamec 2001; Yoder and Kennelly 2003; Venegas et al. 2008). In this paper, the EOF analysis was used to decompose the interannual variability of the chlorophyll-*a* concentration in the South China Sea. The power spectrum of time coefficient functions of the EOF modes were calculated to show the periods of the time coefficient functions.

The data pretreatment method for the EOF analysis includes the following steps: (1) derived the 12 months running mean of the data from the monthly products; (2) the data was log10 transformed as satellite chlorophyll data can be approximated with a lognormal distribution (Campbell et al. 1995); (3) calculated anomaly by subtracting the 111-month mean for each pixel point; and (4)

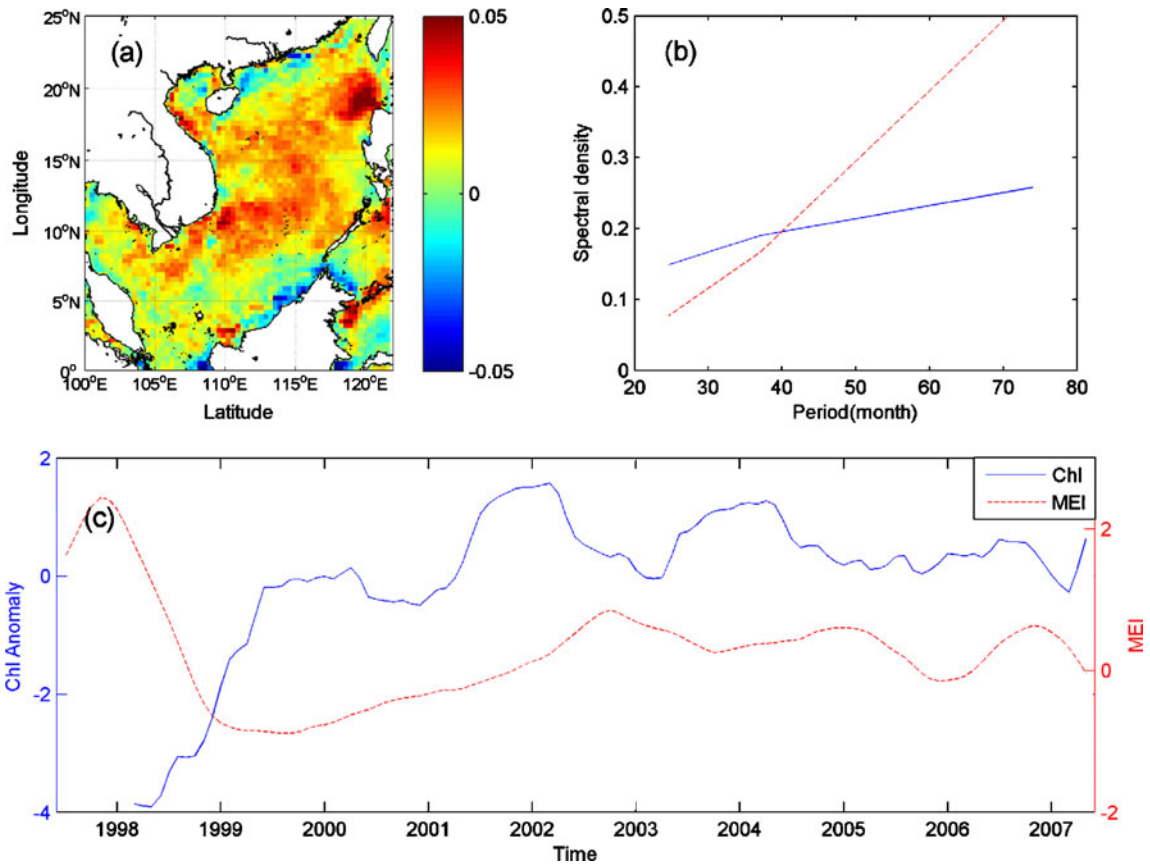

Fig. 3 The first empirical orthogonal function (EOF) mode of the interannual variability of the chlorophyll-*a* concentration in the South China Sea. **a** The distribution of the eigenvector. **b** The *solid blue line* is the power spectrum of the time coefficient function of the EOF mode; the *red dotted line* means in excess of the 95% significance test. **c** The *solid blue line* is the time coefficient function of the EOF mode; the *red dotted line* is the multivariate ENSO index data

weighted every point value using the cosine of latitude (for equal area weighting) to get a data matrix $X_{m\times n}$, where m is the number of spatial points, and n is the time length. The error ranges of the eigenvalues were calculated according to the method of North et al. (1982), $e_j = \lambda_j\sqrt{\frac{2}{n}}$, where e_j is the error range for λ_j.

3 Results

The data after a 12-month running mean was spatially averaged to get the integrated average value for the entire South China Sea. Then, it was compared with MEI (Fig. 2). It is obvious that the chlorophyll-*a* concentration is very low in 1998, and it increases very quickly until 2000. On the whole, the interannual variability of the chlorophyll-*a* concentration is similarly out-of-phase with lags 4 months of MEI.

The interannual variability was analyzed using the EOF. The cumulative variance contribution of the first three EOF modes reached 55.7±7.5%.

The variance contribution of the first mode is 22.2± 3.0% (Fig. 3). Results of the power spectrum of the time coefficient function shows a significant period about 2 to 3 years. The corresponding time coefficient function correlates with the MEI. The correlation coefficient is −0.61 (t<0.0001) when the first time coefficient function lags the MEI by 9 months (Fig. 6a). The eigenvector is more than zero in most of the South China Sea, especially in the deep open water areas. This indicates that the positive time coefficient function of the first EOF mode means the negative MEI (the cold ENSO phase), the chlorophyll-*a* concentration will increase but it will lag the MEI by approximately 9 months, and vice versa. The highest value occurred in the upwelling of the southwest Luzon Strait, which indicates the chlorophyll-*a* concentration significantly diminishes after 9 months of the maturation of the El Niño in the southwest of Luzon Strait.

The variance contribution of the second mode is 21.0± 2.8% (Fig. 4). The analysis of the power spectrum of the time coefficient function shows a significant period about 2 to 6 years. The corresponding time coefficient function

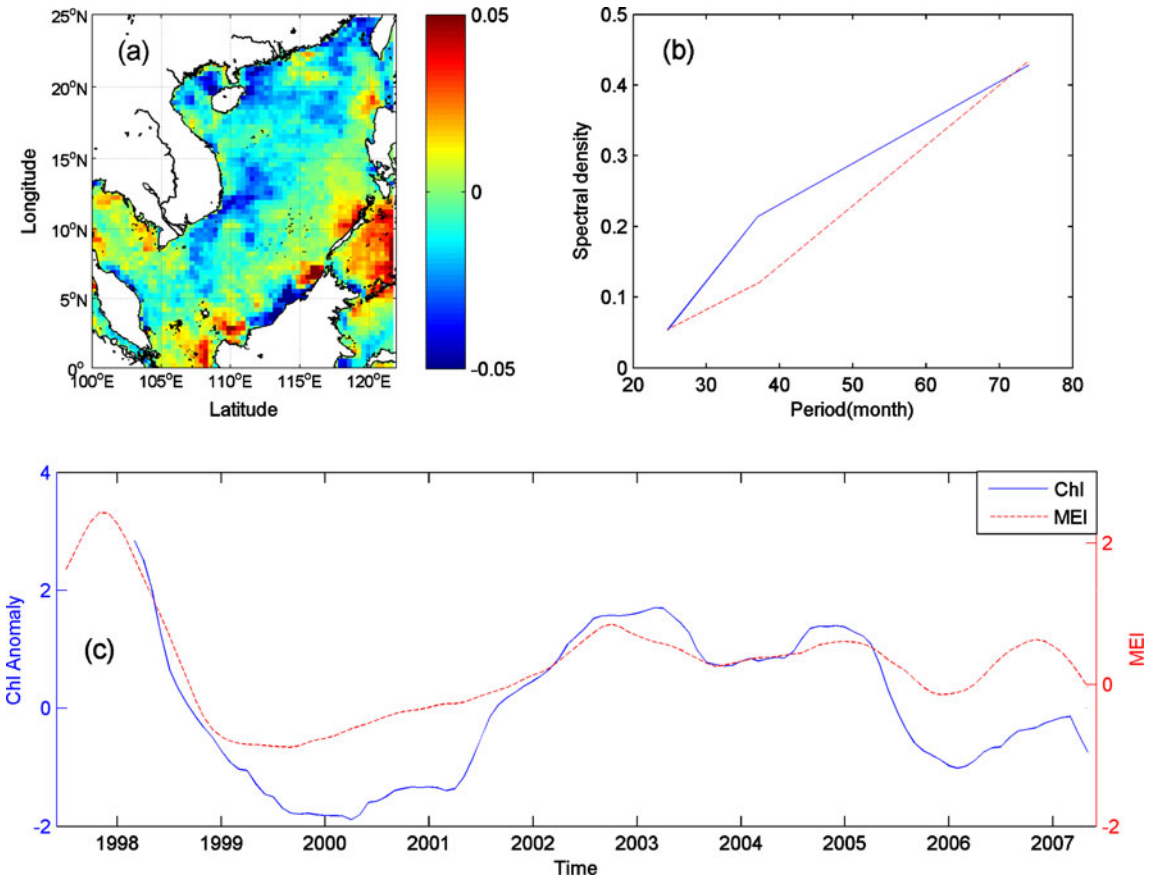

Fig. 4 The second empirical orthogonal function (EOF) mode of the interannual variability of the chlorophyll-*a* concentration in the South China Sea. **a** The distribution of the eigenvector. **b** The *solid blue line* is the power spectrum of the time coefficient function of the EOF mode; the *red dotted line* means in excess of the 95% significance test. **c** The *solid blue line* is the time coefficient function of the EOF mode; the *red dotted line* is the multivariate ENSO index data

highly correlates with the MEI. The correlation coefficient is 0.88 (t<0.0001) when the second time coefficient function lags the MEI by 1 month. Most of the values of the eigenvectors are less than zero, especially in the northwest areas of the South China Sea. That means the chlorophyll-*a* concentration falls over most of the South China Sea within a month of the maturation of the El Niño.

The variance contribution of the third mode is 12.5± 1.7% (Fig. 5). There is no very significant correlation relationship between the time coefficient function of the third mode and the MEI (the highest correlation coefficient is 0.37 with a lag of 1 month). However, it shows a significant correlation relationship with the IOD index. The corresponding coefficient is 0.65 (t<0.0001) when the time coefficient function lags the IOD by 13 months.

4 Conclusion and discussion

The chlorophyll-*a* concentration is one of the most important marine ecological parameters. The ocean dynamic process has an inevitable impact on the marine ecological process. However, there are multiple factors that influence the marine ecosystem, such as light, SST, and nutrients, which make the changes in marine ecology more complex. In this paper, the satellite observation data over the past 10 years were applied to investigate the interannual variability of chlorophyll-*a* distribution in the South China Sea. It was found that the mean interannual variability of the chlorophyll-*a* concentration lags the ENSO by 4 months in the South China Sea.

We found that chlorophyll-*a* concentration is very low in 1998, and it increases very quickly after that period which is in agreement with previous research findings (Zhao and Tang 2007). From 1997 to 1998 is a strong El Niño year, and the SST was found obviously higher than other years in the South China Sea (Fig. 5c of Fang et al. 2006a). Using the EOF analysis method, this paper presented three modes of the EOF decomposition of the interannual chlorophyll-*a* concentration in the South China Sea. It also documents the degree to which their respective time series are correlated to the MEI and the IOD. Two modes were regarded as ENSO-associated modes and the other one was regarded as an IOD-associated mode (Fig. 6).

The interannual chlorophyll-*a* concentration here shows a significant reverse relationship with the interannual variability of SST with a correlation coefficient −0.62 in the South China Sea (Fig. 7a). Behrenfeld et al. observed

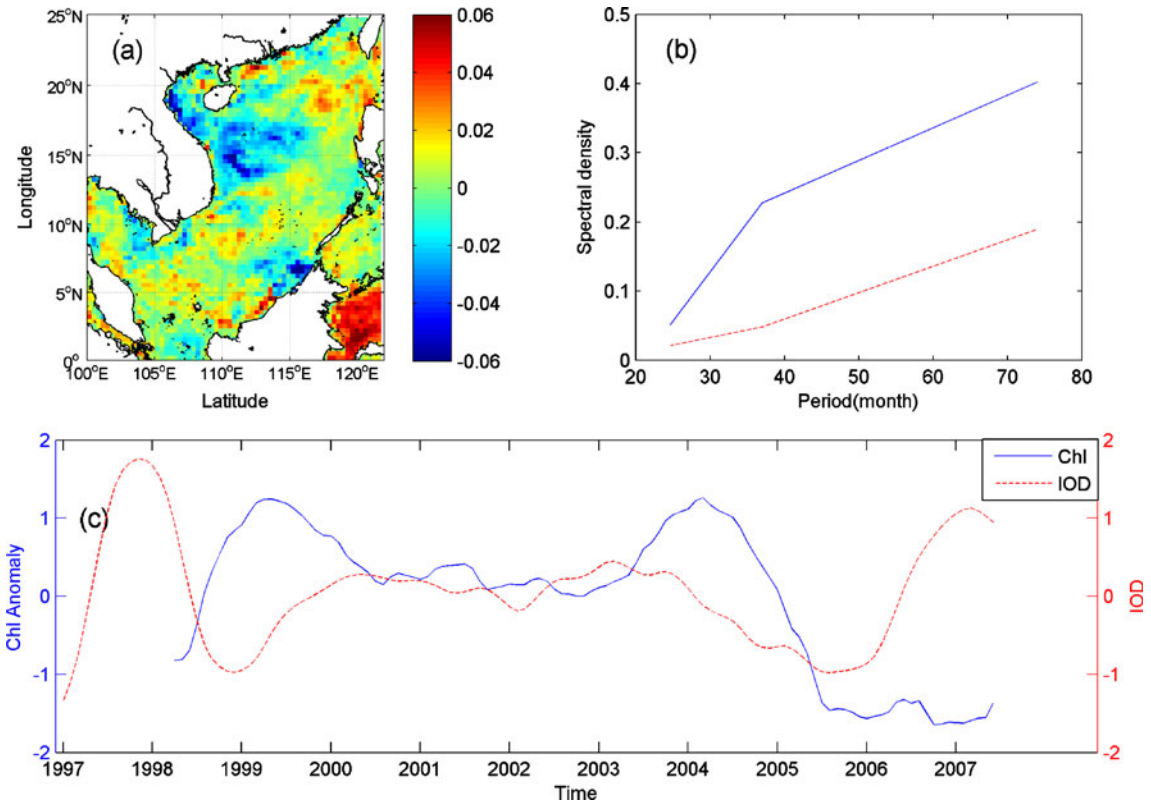

Fig. 5 The third empirical orthogonal function (EOF) mode of the interannual variability of the chlorophyll-*a* concentration in the South China Sea. **a** The distribution of the eigenvector. **b** The *solid blue line* is the power spectrum of the time coefficient function of the EOF mode; the *red dotted line* means in excess of the 95% significance test. **c** The *solid blue line* is the time coefficient function of the EOF mode; the *red dotted line* is the Indian Ocean dipole index data

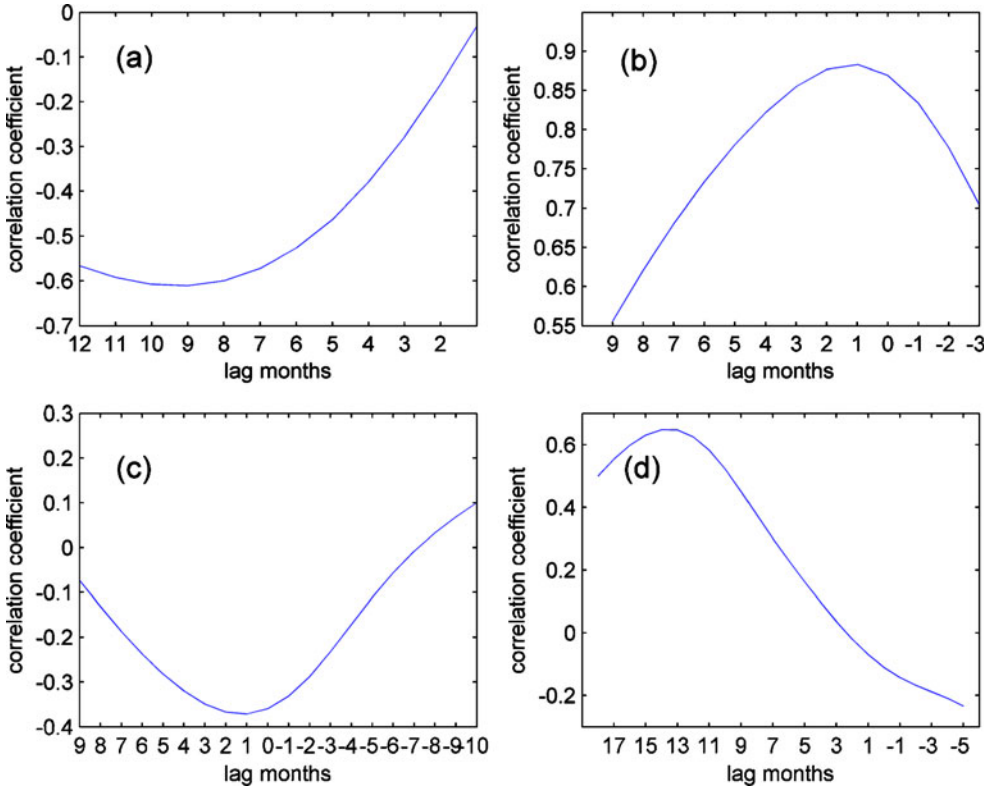

Fig. 6 The correlation relationship of time coefficient functions with the multivariate ENSO index (MEI) or Indian Ocean dipole (IOD) index when lags different months. **a** The time coefficient function of the empirical orthogonal function (EOF) 1 mode and the MEI. **b** The time coefficient function of the EOF 2 mode and the MEI. **c** The time coefficient function of the EOF 3 mode and the MEI. **d** The time coefficient function of the EOF 3 mode with the IOD index

that as the SST increase, the photosynthetic rate increases between −1°C and 20°C and subsequent decreases at temperature >20°C (Fig. 7 of Behrenfeld and Falkowski 1997). The higher SST accompanied with lower chlorophyll-*a* concentration in the South China Sea does not mean temperature itself directly influence the photosynthetic rate of the phytoplankton. However, the effect of the SST on the nutrient stress and mixed layer light level may lead to correlation between SST and photosynthetic rate. Here, the interannual chlorophyll-*a* concentration also shows a relationship with wind stress curl with a correlation coefficient equal to 0.62 (Fig. 7b). The wind stress

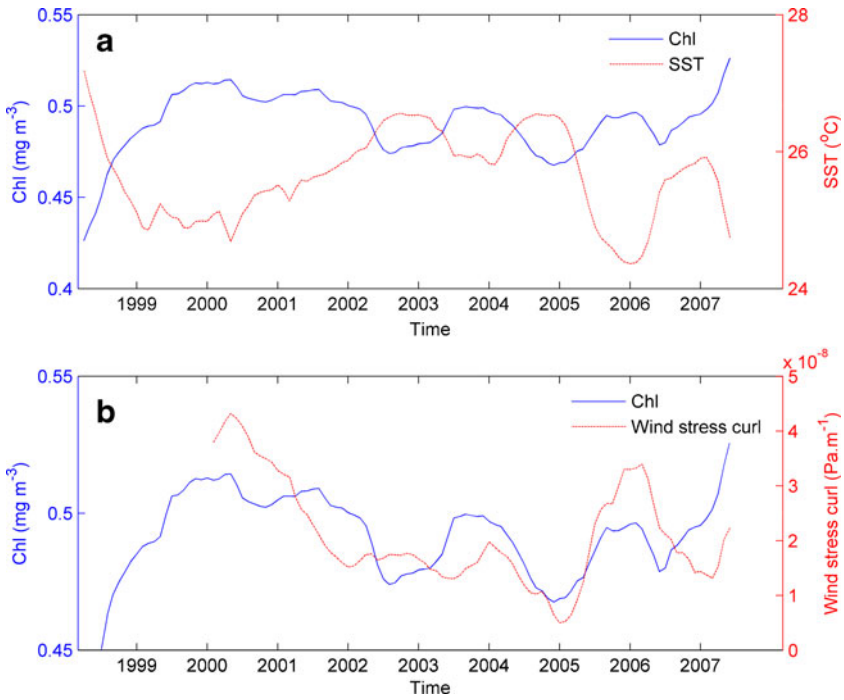

Fig. 7 The relationship between the interannual chlorophyll-*a* concentration and interannual SST (**a**), and the relationship between the interannual chlorophyll-*a* concentration and interannual wind stress curl (**b**)

influence on the stratification of the water column. The Ekman pumping induced by the wind stress curl will induce the seawater upwelling with more nutrients.

The time coefficient function of the first EOF mode lags the MEI by 9 months, and the time coefficient function of the second EOF mode lags the MEI by 1 month. The first two EOF modes' chlorophyll-*a* concentration evolution may be associated with two peaks in SST following an El Niño event (Wang et al. 2006).

The first and the second EOF modes illustrate that the chlorophyll-*a* concentration will become lower after the mature phrase of the El Niño. A double-trough chlorophyll-*a* concentration evolution will appear following an El Niño event. One is after 1 month, and the other is after 9 months of the mature phrase of the El Niño. In the first EOF mode, the obvious high value area is the southwest of Luzon Strait, which is always called Luzon cold-core eddy. The Luzon cold eddy always appears in winter and spring, and phytoplankton was found blooming in winter in those areas (Tang et al. 1999). The weakening of the northeast monsoon during the El Niño period in the northern South China Sea, including the Luzon Strait, brings less cold water into and less cold and dry air over the South China Sea. This leads to a higher SST anomaly following the El Niño. The greatest warming appears in the northern deep basin, located in the Luzon cold eddy areas. During the 1998 El Niño event, the monsoon winds weakened the upwelling and resulted in the mean SST in the study area being 0.8°C higher than the 4-year average from 1997 to 2000 (Kuo et al. 2004). Wang et al. reported the shortwave radiation and latent heat flux anomalies, which led to a rising SST in February after the mature phrase of El Niño (Wang et al. 2006). Moreover, in August after the mature phrase of the El Niño, the mean meridional geostrophic heat advection makes the South China SST rise again (Wang et al. 2006).

The third EOF mode implies that there is a correlation between the chlorophyll-*a* variability and the IOD index. The time coefficient function of the third EOF mode lags the IOD index by 13 months, which indicates that the chlorophyll-*a* concentration anomaly in the South China Sea is also influenced by the IOD.

The dependence/independence of the IOD and the El Niño/Southern Oscillation (ENSO) phenomena has some controversy. Some researches suggested that although the IOD is independent of the ENSO in some years, but overall, there are some close connections through the Walker circulation across the tropical Indo-Pacific Ocean (Chao et al. 2005). Recent research has indicated that the IOD is influenced by the ENSO event in some years, but the ENSO is not the only triggering mechanism (Saji et al. 2006).

The IOD impacts the Asian summer monsoon activities. A normal (late) South China Sea summer monsoon onset is associated with the previous positive (negative) IOD. A negative IOD results in a delayed monsoon onset and a normal onset after each positive IOD (Yuan et al. 2008). The monsoon causes the mixture of the water then brings abound of nutrient to the surface for the phytoplankton growth.

This study analyzed the interannual variability of the chlorophyll-*a* concentration and its relationship with the ENSO and the IOD in the South China Sea for the first time. It offers some references on the marine ecological variability analysis for other sea areas.

Acknowledgments This work was supported by the National Basic Research Program of China (973 Program; 2009CB723903), National Natural Science Foundation of China (40676096), and 863-Project (2009AA12Z102-10). We thank OBPG of the GSFC, NASA for providing SeaWiFS chlorophyll-*a* products, Physical Oceanography Distributed Active Archive Centre (PODAAC) at the NASA Jet Propulsion Laboratory for providing AVHRR SST data, and CERSAT at the Ifremer for providing the QuikSCAT products. Thanks to Kelly Hille who helped us edit the manuscript. We also thank three anonymous reviewers for their thorough reviews and constructive comments.

References

Behrenfeld MJ, Falkowski PG (1997) Photosynthetic rates derived from satellite-based chlorophyll concentration. Limnol Oceanogr 42(1):1–20

Behrenfeld MJ, O'Malley RT, Siegel DA, McClain CR, Sarmiento JL, Feldman GC, Milligan AJ, Falkowski PG, Letelier RM, Boss ES (2006) Climate-driven trends in contemporary ocean productivity. Nature 444:752–755

Campbell JW, Blaisdell JM, Darzi M (1995) Level-3 SeaWiFS data products: spatial and temporal binning algorithms. In: Hooker SB, Firestone ER (eds) NASA technical memorandum 104566 vol. 32. NASA Goddard Space Flight Center, USA

Chao J, Chao Q, Liu L (2005) The ENSO events in the tropical Pacific and Dipole events in the Indian Ocean. Acta Meteor Sinica 63:594–602

Emery WJ, Thomson RE (2001) Data analysis and methods in physical oceanography. Elsevier, New York

Fang GH, Chen HY, Wei ZX, Wang YG, Wang XY, Li CY (2006a) Trends and interannual variability of the South China Sea surface winds, surface height, and surface temperature in the recent decade. J Geophys Res Oceans 111:16

Fang WD, Guo JJ, Shi P, Mao QW (2006b) Low frequency variability of South China Sea surface circulation from 11 years of satellite altimeter data. Geophys Res Lett 33:5

Han G, Huang W (2009) Low-frequency sea-level variability in the South China Sea and its relationship to ENSO. Theor Appl Climatol 97:41–52

Ho CR, Zheng QN, Soong YS, Kuo NJ, Hu JH (2000) Seasonal variability of sea surface height in the South China Sea observed with TOPEX/Poseidon altimeter data. J Geophys Res Oceans 105:13981–13990

Hooker SB, McClain CR (2000) The calibration and validation of SeaWiFS data. Prog Oceanogr 45:427–465

Kuo N-J, Zheng Q, Ho C-R (2004) Response of Vietnam coastal upwelling to the 1997-1998 ENSO event observed by multi-sensor data. Remote Sens Environ 89:106–115

Legaard KR, Thomas AC (2007) Spatial patterns of intraseasonal variability of chlorophyll and sea surface temperature in the California current. J Geophys Res Oceans 112:19

Li YC, Li L, Jing CS, Cai WL (2004) Temporal and spatial variabilities of sea surface heights in the northeastern South China Sea. Chin Sci Bull 49:491–498

Li W, Wang D, Lei T, Wang H (2009) Convective and stratiform rainfall and heating associated with the summer monsoon over the South China Sea based on TRMM data. Theor Appl Climatol 95:157–163

Liu HB, Chang J, Tseng CM, Wen LS, Liu KK (2007) Seasonal variability of picoplankton in the northern South China Sea at the SEATS station. Deep Sea Res II 54:1602–1616

Nagar SG, Singh SV (1991) Variations of surface pressure over India during the southwest monsoon. Theor Appl Climatol 44:95–112

North GR, Bell TL et al (1982) Sampling errors in the estimation of empirical orthogonal functions. Mon Weather Rev 110(7):699–706

Penaflor EL, Villanoy CL, Liu CT, David LT (2007) Detection of monsoonal phytoplankton blooms in Luzon Strait with MODIS data. Remote Sens Environ 109:443–450

Qu TD (2001) Role of ocean dynamics in determining the mean seasonal cycle of the South China Sea surface temperature. J Geophys Res Oceans 106:6943–6955

Saji NH, Goswami BN, Vinayachandran PN, Yamagata T (1999) A dipole mode in the tropical Indian Ocean. Nature 401:360–363

Saji NH, Xie SP, Yamagata T (2006) Tropical Indian Ocean variability in the IPCC twentieth-century climate simulations. J Clim 19:4397–4417

Shen S, Leptoukh GG, Acker JG, Yu Z, Kempler SJ (2008) Seasonal variations of chlorophyll a concentration in the northern South China Sea. IEEE Geosci Remote Sens Lett 5(2):315–319

Stein ML (1999) Interpolation of spatail data: theory for kriging. Springer, Berlin

Tan CK, Ishizaka J, Matsumura S, Yusoff FM, Mohamed MIH (2006) Seasonal variability of SeaWiFS chlorophyll a in the Malacca Straits in relation to Asian monsoon. Cont Shelf Res 26:168–178

Tang DL, Ni IH, Kester DR, Muller-Karger FE (1999) Remote sensing observations of winter phytoplankton blooms southwest of the Luzon Strait in the South China Sea. Mar Ecol Prog Ser 191:43–51

Tang S, Chen C, Zhan H, Zhang J, Yang J (2008) An appraisal of surface chlorophyll estimation by satellite remote sensing in the South China Sea. Int J Remote Sens 29:6217–6226

Venegas RM, Strub PT, Beier E, Letelier R, Thomas AC, Cowles T, James C, Soto-Mardones L, Cabrera C (2008) Satellite-derived variability in chlorophyll, wind stress, sea surface height, and temperature in the northern California current system. J Geophys Res Oceans 113:C03015

Wang DX, Liu Y, Qi YQ, Shi P (2001) Seasonal variability of thermal fronts in the northern South China Sea from satellite data. Geophys Res Lett 28:3963–3966

Wang CZ, Wang WQ, Wang DX, Wang Q (2006) Interannual variability of the South China Sea associated with El Nino. J Geophys Res Oceans 111:19

Wilson C, Adamec D (2001) Correlations between surface chlorophyll and sea surface height in the tropical Pacific during the 1997-1999 El Nino-Southern Oscillation event. J Geophys Res Oceans 106:31175–31188

Wolter K, Timlin SM (1993) Monitoring ENSO in COADS with a seasonally adjusted principal component index. Proceedings of the Seventh Annual Climate Diagnostic Workshop, Norman, Oklahoma

Wolter K, Timlin MS (1998) Measuring the strength of ENSO events—how does 1997/98 rank? Weather 53:315–324

Yoder JA, Kennelly MA (2003) Seasonal and ENSO variability in global ocean phytoplankton chlorophyll derived from 4 years of SeaWiFS measurements. Glob Biogeochem Cycles 17:1112

Yuan Y, Yang H, Zhou W, Li CY (2008) Influences of the Indian Ocean dipole on the Asian summer monsoon in the following year. Int J Climatol 28:1849–1859

Zeng L, Wang D (2009) Intraseasonal variability of latent-heat flux in the South China Sea. Theor Appl Climatol 97:53–64

Zhao H, Tang DL (2007) Effect of 1998 El Nino on the distribution of phytoplankton in the South China Sea. J Geophys Res-Oceans 112:8

Zhao H, Qi YQ, Wang DX, Wang WZ (2005) Study on the features of chlorophyll-a derived from SeaWiFS in the South China Sea. Acta Oceanol Sinica 27:45–52